NAVAL POSTGRADUATE SCHOOL

MONTEREY, CALIFORNIA

THESIS

THE INTERACTION OF WAKES GENERATED BY SUBMERGED PROPAGATING OBJECTS WITH THE TURBULENT SUBSURFACE MIXED LAYER

by

Hwanhee Lee

March 2022

Thesis Advisor: Timour Radko
Second Reader: Justin M. Brown

THIS PAGE INTENTIONALLY LEFT BLANK

REPORT DOCUMENTATION PAGE			*Form Approved OMB No. 0704-0188*

1. AGENCY USE ONLY *(Leave blank)*	**2. REPORT DATE** March 2022	**3. REPORT TYPE AND DATES COVERED** Master's thesis

4. TITLE AND SUBTITLE
THE INTERACTION OF WAKES GENERATED BY SUBMERGED PROPAGATING OBJECTS WITH THE TURBULENT SUBSURFACE MIXED LAYER

5. FUNDING NUMBERS

6. AUTHOR(S) Hwanhee Lee

7. PERFORMING ORGANIZATION NAME(S) AND ADDRESS(ES)
Naval Postgraduate School
Monterey, CA 93943-5000

8. PERFORMING ORGANIZATION REPORT NUMBER

9. SPONSORING / MONITORING AGENCY NAME(S) AND ADDRESS(ES)
N/A

10. SPONSORING / MONITORING AGENCY REPORT NUMBER

11. SUPPLEMENTARY NOTES The views expressed in this thesis are those of the author and do not reflect the official policy or position of the Department of Defense or the U.S. Government.

12a. DISTRIBUTION / AVAILABILITY STATEMENT
Approved for public release. Distribution is unlimited.

12b. DISTRIBUTION CODE
A

13. ABSTRACT (maximum 200 words)

In this study, the numeral simulations were conducted using OpenFOAM to investigate how changes in mixed layer depth (MLD), speed and depth of a submerged body (SB) affect observable signatures of the SB moving beneath a mixed layer. We studied the effect of these factors on both surface and interior temperature perturbations. This study has shown that the wake generated by an SB in the presence of a mixed layer has a greater surface temperature signature than that without it. Furthermore, the deeper the MLD, the greater the thermal signal. This is because when the mixed layer is present, the region is more weakly stratified than it would be without a mixed layer, and the reduced buoyancy force permits fluid entering the mixed layer to penetrate farther. Through variation in speed and depth of SB, we found that faster SB results in stronger turbulence, greater temperature change, and larger areas of surface wake penetration. Also, deeper SB motion levels result in greater surface temperature signals by dredging up colder water from the SB surroundings to the surface. This study confirmed the possibility of detection through surface temperature changes formed by wakes inevitably generated by submerged objects.

14. SUBJECT TERMS
anti-submarine warfare, turbulent wakes, the interaction of wakes, submerged propagating objects, subsurface mixed layer, surface thermal signatures, high-resolution numerical simulations, submerged body, SB, mixed layer depth, MLD

15. NUMBER OF PAGES
49

16. PRICE CODE

17. SECURITY CLASSIFICATION OF REPORT	**18. SECURITY CLASSIFICATION OF THIS PAGE**	**19. SECURITY CLASSIFICATION OF ABSTRACT**	**20. LIMITATION OF ABSTRACT**
Unclassified	Unclassified	Unclassified	UU

NSN 7540-01-280-5500

Standard Form 298 (Rev. 2-89)
Prescribed by ANSI Std. 239-18

THIS PAGE INTENTIONALLY LEFT BLANK

Approved for public release. Distribution is unlimited.

THE INTERACTION OF WAKES GENERATED BY SUBMERGED PROPAGATING OBJECTS WITH THE TURBULENT SUBSURFACE MIXED LAYER

Hwanhee Lee
Dae-wi, Republic of Korea Navy
MMAS, Korea Naval Academy, 2013

Submitted in partial fulfillment of the
requirements for the degree of

MASTER OF SCIENCE IN PHYSICAL OCEANOGRAPHY

from the

NAVAL POSTGRADUATE SCHOOL
March 2022

Approved by: Timour Radko
Advisor

Justin M. Brown
Second Reader

Peter C. Chu
Chair, Department of Oceanography

THIS PAGE INTENTIONALLY LEFT BLANK

ABSTRACT

In this study, the numeral simulations were conducted using OpenFOAM to investigate how changes in mixed layer depth (MLD), speed and depth of a submerged body (SB) affect observable signatures of the SB moving beneath a mixed layer. We studied the effect of these factors on both surface and interior temperature perturbations. This study has shown that the wake generated by an SB in the presence of a mixed layer has a greater surface temperature signature than that without it. Furthermore, the deeper the MLD, the greater the thermal signal. This is because when the mixed layer is present, the region is more weakly stratified than it would be without a mixed layer, and the reduced buoyancy force permits fluid entering the mixed layer to penetrate farther. Through variation in speed and depth of SB, we found that faster SB results in stronger turbulence, greater temperature change, and larger areas of surface wake penetration. Also, deeper SB motion levels result in greater surface temperature signals by dredging up colder water from the SB surroundings to the surface. This study confirmed the possibility of detection through surface temperature changes formed by wakes inevitably generated by submerged objects.

THIS PAGE INTENTIONALLY LEFT BLANK

TABLE OF CONTENTS

THIS PAGE INTENTIONALLY LEFT BLANK

LIST OF FIGURES

LIST OF TABLES

THIS PAGE INTENTIONALLY LEFT BLANK

LIST OF ACRONYMS AND ABBREVIATIONS

ASW	Anti Submarine Warfare
CFD	Computational Fluid Dynamics
ML	Mixed Layer
MLD	Mixed Layer Depth
SB	Submerged Body
SLD	Sonic Layer Depth

THIS PAGE INTENTIONALLY LEFT BLANK

ACKNOWLEDGMENTS

First of all, I'd like to thank Dr. Timour Radko. He was always kind and energetic while guiding me throughout the entire period. Also, I would like to thank Dr. Justin Brown for constantly educating me about CFD and giving me directions to move forward. I would also like to thank all the super-computing managers, especially Jeff Haferman, for their systematic support to make the most of Hamming (High Performance Computing) for this study.

Secondly, I would like to thank Singapore Navy Major Dexter, Tan and Taiwan Navy Lieutenant Shen, Yi-fan for being true friends and classmates beyond nationality.

Lastly, I want to say thank you to my lovely family. I would like to thank my son, Harang Lee, who always makes me happy with his cute smile and lovely behavior. He is a 3-year-old child who doesn't even know where we are yet, but he always went to daycare centers bravely and stayed healthy even on a long trip. And I would like to thank my lovely wife, Soyun Kwag, who always took care of the family with love and supported me so I could concentrate on my studies. I would never have completed this paper without her dedicated support.

THIS PAGE INTENTIONALLY LEFT BLANK

I. INTRODUCTION

A. MOTIVATION

Typically, submarines are detected acoustically. However, acoustic detection methods suffer from several key problems, ranging from advancements in submarine masking technology to particular oceanographic features that interfere with acoustic detection. Some technological advancements—including sound-absorbing outer coating and ultra-quiet air-independent propulsion systems—have rendered the acoustics-based techniques less effective. In addition, the surface mixed layer can shield submersibles from surface acoustic detection. These shortcomings motivate the search for alternative detection and tracking methods, some of which involve the identification of turbulent wakes that are inevitably generated by propagating solid objects in the ocean. This study focuses on how submerged wakes below the mixed layer produce temperature signals at the surface and turbulence near the path of the submerged body.

The mixed layer is one oceanographic feature that hiders acoustic detection. The mixed layer is defined as a layer nearly vertically uniform in salinity, temperature, and density and is generated by wind and buoyancy forcing. Within a mixed layer, sound is refracted upward because the density decreases with depth, and in the upper regions of the thermocline (which is typically located beneath the mixed layer), the sound is refracted downward as the density increases with depth. This sound speed profile generates a "shadow zone," where active sonar from a surface vessel cannot reach, and objects within this zone become virtually undetectable by acoustic means.

Given the issues plaguing direct acoustic detection, it is possible instead to use other indirect methods, such as searching for the submarine's wake. All objects traveling through fluid leave wakes and various studies have been conducted on wake evolution and detectability. This method was discussed, for instance, by Spedding et al. (1996), and entire area of research is summarized in Spedding (2014). However, little work has been done to date on how turbulent wakes interact with an adjacent mixed layer, and such an environment is particularly problematic for acoustic detection for the reasons outlined

above. If the turbulence from the wake under the mixed layer may induce thermal mixing and this mixing can extend to the surface, such signals could be detected on planes via infrared imagery. It is thus prudent to investigate how far submerged wakes extend vertically for use in naval anti-submarine warfare (ASW). To address these issues, this study focuses on the ability of the wake to penetrate the mixed layer and quantifies the surface thermal signatures of a submarine.

B. BACKGROUND

Stratification has an important role in the development and decay of turbulence. Many studies have been conducted on this subject. Lin and Pao (1973) observed the generation and decay of turbulence by using a cylinder in a stratified salty water tank and showed the effect of stratification on the evolution of turbulent flow using a grid. They showed that the wake becomes flattened as it develops, and this flattened wake is resilient to decay. Similarly, Lin and Veenhuizen (1974) performed laboratory experiments of grid-generated turbulence and showed that vertical motion damps more quickly in a stratified system. Pao (1973) and Lin and Veenhuizen (1974) both address that vertical motion of wake is more suppressed within the stratified fluid. Spedding (1997) classified stratified wakes into three stages: 3D, non-equilibrium, and quasi-2D, which we refer to as the "near," "intermediate," and "far-field" wake stages, respectively. During the near wake, the turbulence in the wake is strong, and the flow extends roughly homogenously in all directions (Spedding, 2002). As the wake transitions to the intermediate stage, the effects of buoyancy start to become more prominent, and this serves to flatten and collapse the wake vertically as it comes to a level of neutral buoyancy (Schooley & Stewart, 1963). Finally, the far-field wake shows the development of flattened "pancake vortices" and continues to expand in the horizontal direction while remaining roughly flat in the vertical. Meunier and Spedding (2004) maneuvered SBs of various sizes and shapes within the stratified fluid and showed that neither the structure of the intermediate nor the far wake appeared to depend strongly on the initial shape of the body. For detection, it is most relevant to investigate the later stages of the wake, but such simulations are infeasible at present. Thus, this study focuses on the near wake.

Prior research has shown that wake signatures are detectable in a variety of ways. Spedding (1996) conducted studies of a wake in a stratified tank, and these results can be extrapolated to oceanographic parameters to suggest that signatures generated by submersibles should be identifiable for several days. Radko and Lewis (2019) analyzed the decay of a wake numerically, using the turbulent and thermal dissipation rates, which suggested that a wake created by a SB 10m in diameter with a speed of 10m/s could be detected over several hours. For surface thermal signatures, Voropayev et al. (2012) showed that a propeller-driven model ship produced a detectable surface temperature in a stratified tank. Voropayev et al. (2007) and Moody et al. (2017) also showed the turbulence created by a SB makes a detectable signal on the surface using laboratory experiments. For wake signatures in stratified fluids, it is prudent to focus on what fundamental parameters determine the strength of these signatures.

The Froude number is normally used to characterize stratified wakes:

$$\mathrm{Fr} = \frac{U}{NL}, \tag{1.1}$$

where U and L are the submerged body's speed and size, respectively, and $N = \sqrt{\beta_T g(\partial T / \partial z)}$ is the Brunt–Väisälä frequency, and β_T, g, $\partial T / \partial z$ are the thermal expansion coefficient, the acceleration due to gravity, and the vertical gradient of temperature. For Fr < 1, the flow is subcritical: the buoyancy force dominates the flow and causes the wake to collapse rapidly. For Fr > 1, the flow is supercritical: inertial forces dominate. The larger Fr means that the buoyancy timescale becomes much longer, so the effects of stratification are less pronounced at early times. The stratified wake expands vertically and laterally as it would without stratification, and the vertical wake collapse proceeds afterwards. For submarines operating in the ocean, Fr is typically in the range of 100–300. Spedding (2014) noted that the dependence of the wake signature on Fr is fairly small at any given non-dimensional time (Nt) after the initial passage of the body. This suggests that stratified wakes, especially in later stages, are not sensitive to the initial shape of the body.

The strength of the turbulence in a wake is largely determined by the Reynolds number of the flow:

$$\mathrm{Re} = \frac{UL}{v}, \tag{1.2}$$

where v is the kinematic viscosity. For low Re (less than 10^3), the flow is laminar, while for high Re, the flow is turbulent. The Reynolds number is significant because it determines the initial amount of turbulence generated by the body. For submarines, the Reynolds number is typically large, on the order of 10^8 for typical operational conditions. Brucker & Sarkar (2010) showed the non-equilibrium regime of wake evolution is longer for higher Reynolds numbers. Diamessis et al. (2011) compared the non-equilibrium stage of the wake at a relatively lower Re ($5 \cdot 10^3$) and a higher Re (10^5) and showed that the wake persisted for longer at higher Re, while the vertical motion of the wake was more rapidly suppressed at a lower Re.

C. APPROACH

This thesis addresses the problem of the interaction of wakes generated by submerged propagating objects with the turbulent subsurface mixed layer. Particular attention is given to the ability of the wake to penetrate the mixed layer, which ultimately controls the surface thermal signatures of a submarine. The project involves a series of numerical experiments, in which we systematically vary both the properties of the wake-generating object (speed and depth) and the depth of the mixed layer and then analyze the temperature signatures at surface and turbulence signatures at depth. In this study, we find that the wake generated by a SB beneath a mixed layer has a greater surface temperature signature than that without a mixed layer, and the deeper the MLD, the greater the temperature change. In addition, in variation in speed and depth of SB experiments, we find that faster SB speed results in stronger turbulence, greater temperature change and larger areas of surface wake penetration. Deeper SB trajectories result in greater surface temperature signals by dredging up colder water from the SB surroundings to the surface.

In Chapter II, we describe our modeling setup and methodology. In Chapter III, our results are presented based on the results of thermal changes and decay rates of the wake signals. In Chapter IV, we discuss our conclusions, the operational relevance of our research, and provide recommendations for future research opportunities.

THIS PAGE INTENTIONALLY LEFT BLANK

II. METHODS

A. NUMERICAL MODEL

We conduct high-resolution numerical simulations using OpenFOAM (v2106), which is an open-source CFD (Computational Fluid Dynamics) software (Weller et al., 1998). This model is chosen because it has a wide range of capabilities important for wake modeling, including dynamic meshing, turbulence modeling, and the ability to resolve the boundary layer near solid walls. This study uses LES (Large Eddy Simulations), which separate the fluid equations into large-scale and small-scale turbulence. The small-scale turbulence, which is smaller than a single grid cell, is modeled and typically appears in the governing equations as a dissipative term. This way, the large-scale turbulence modeled explicitly is mixed by the small-scale turbulence modeled parametrically. We use the Spalart-Allmaras Delayed DES (Detached Eddy Simulation) formulation (Spalart et al., 1997), which is generally used for flows bounded by solid walls.

This study uses the Boussinesq approximation. That is, the density perturbation away from a constant reference density, ρ_0, is a linear function of temperature and only impacts the buoyancy term in the momentum equation. We ignore the effects of planetary rotation and external forcing, which is justified because the wake timescale is much shorter than the planetary rotation timescale. In the absence of external forcing, we focus here on a thermally driven mixed layer to generate the simplest possible scenario for a driven mixed layer. The governing equations are described by Equations 2.1 through 2.4.

$$\frac{\partial \mathbf{u}}{\partial t} + \mathbf{u} \cdot \nabla \mathbf{u} = -\frac{1}{\rho_0} \nabla p + g \beta_T (T - T_{ref}) \vec{k} + (\nu + \nu_t) \nabla^2 \mathbf{u} \tag{2.1}$$

$$\frac{\partial T}{\partial t} + \mathbf{u} \cdot \nabla T = (K_T + \nu_t / \mathrm{Pr}_t) \nabla^2 T \,, \tag{2.2}$$

$$\nabla \cdot \mathbf{u} = 0 \,, \tag{2.3}$$

$$\frac{\rho - \rho_0}{\rho_0} = -\beta_T (T - T_{ref}) \,, \tag{2.4}$$

where $\mathbf{u} = (u, v, w)$ is the total velocity vector, $\vec{k}$ is the vertical unit vector, p is the pressure, ρ is the density, T is the sea-water temperature, and T_{ref} is a reference temperature, which is set to be the typical sea surface temperature. The thermal expansion coefficient, β_T, is set to $0.5\times10^{-4}\,^{\circ}\mathrm{C}^{-1}$, the gravitational acceleration, g, is set to 9.81m/s^2, the kinematic viscosity, ν, is set to 1×10^{-6} m^{-2}s^{-1} and ν_t is the turbulent viscosity (which is determined by the LES scheme). The turbulent Prandtl number, Pr_t, is set to 1, the molecular diffusivity of heat, K_T, is set to 1.4×10^{-7} m^2/s and the reference density, ρ_0, is set to 1024 kg/m^3.

B. EXPERIMENTAL CONFIGURATION

Figure 1 depicts the geometry of the model. The domain is a rectangular box of size 700m x 200m x 220m in x, y, and z respectively. Within this domain, a 10-m body translates in the positive *x* direction. As shown in Figure 2, the domain depth of the wake simulations is divided into two regions: the upper 70m and lower 150m. The upper region, which includes the submerged body, is resolved with 1m grid increment in all directions. This is where the wake is most prominent and therefore requires the highest resolution. The lower region has the same horizontal resolution, but the vertical grid spacing increases exponentially from 1m near the top to 9m near the bottom, where there is very little motion. The top boundary is impermeable and free-slip, and the bottom boundary allows for outflows by setting the normal gradients of *T* and **u** to be zero. The left, right, forward, and back boundary conditions are periodic. The pressure is zero on the bottom boundary, with the normal gradient set to zero at the top boundary.

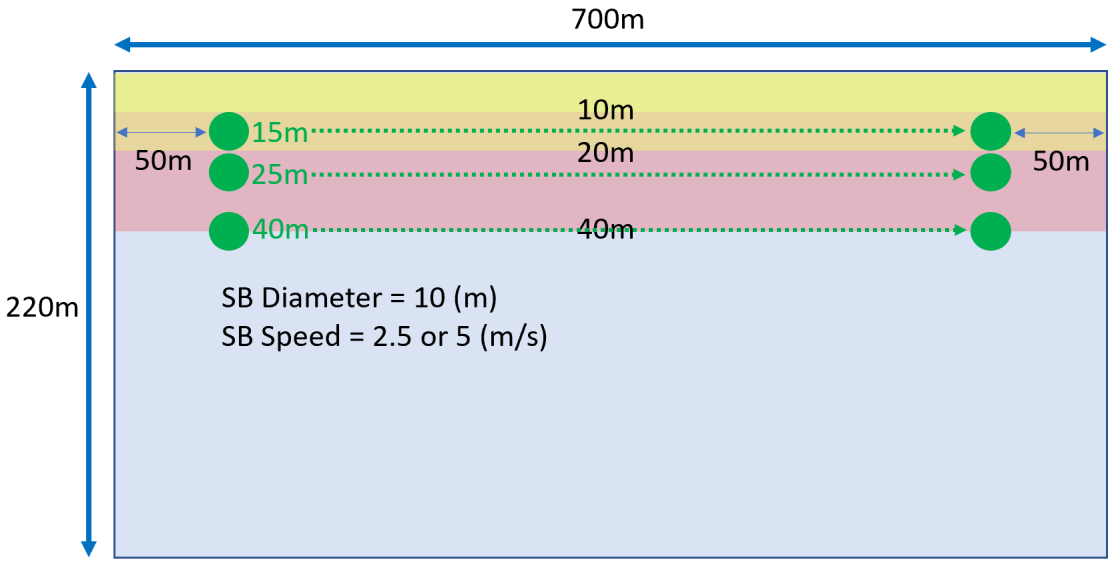

Figure 1. Schematic diagram of the model configuration. Shown is the vertical (x,z) section

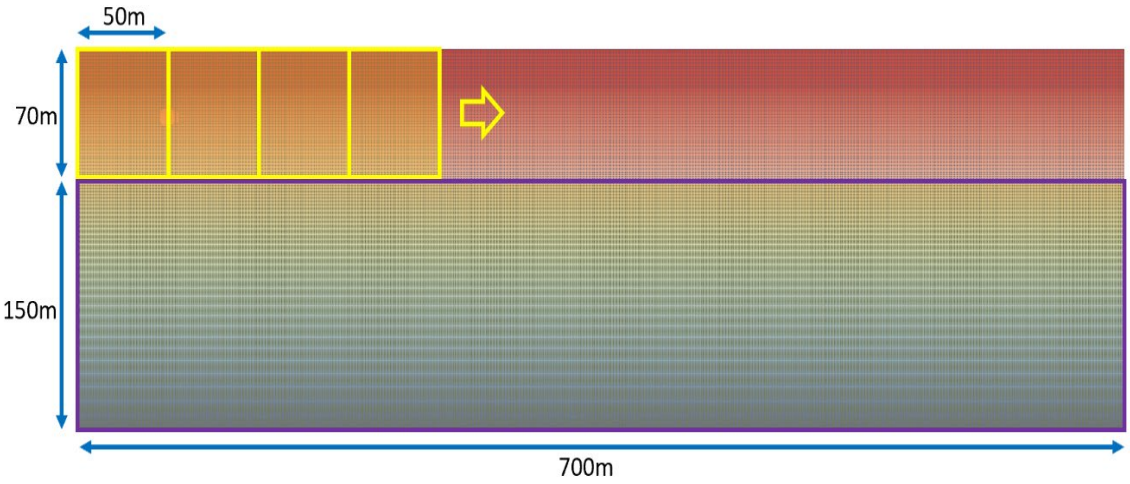

Figure 2. Schematic illustrating the numerical outer mesh and the tiled model of the mixed layer.

The initial conditions for the simulation are created by allowing a mixed layer to develop naturally in a smaller, periodic domain. A smaller domain is used for the initial condition because the mixed layer evolution timescale (on the order of days) is much longer than the wake timescale (on the order of minutes), and this makes the initial conditions prohibitively expensive to evaluate for the full domain. The surface boundary

for these initial simulations is forced by setting the mean temperature at the surface as follows,

$$\overline{T} = T_0 \sin(\omega t), \tag{2.5}$$

where ω is the angular frequency of the Earth's rotation (7.2722e-05s $^{-1}$). The amplitude of the oscillation is T_0, which is calibrated to yield the desired mixed layer depth: 0.4ºC for 10m, 1.0ºC for 20m, and 2.0ºC for 40m. The initial simulation is evolved for a week, and the result is tiled in x and y as indicated in Figure 2 by the yellow rectangles to form the initial condition for the wake simulations. The lower domain is initialized with a uniform temperature gradient instead. The final temperature profile produced by this initial simulation is illustrated in Figure 3. This plot represents the initial condition of the 20 m mixed layer case, so the temperature from the surface to the bottom of the mixed layer remains constant at about 0 °C and then rapidly cools down from the bottom of the mixed layer.

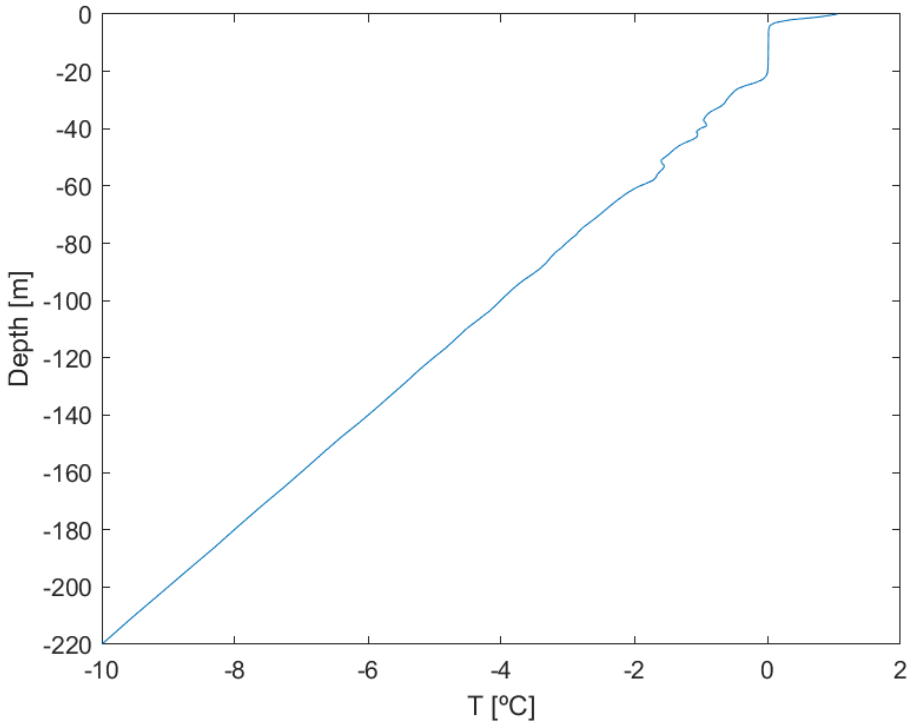

Figure 3. The temperature profile used as the initial condition for the simulation with 20m mixed layer.

The domain is split into an “inner mesh” and an “outer” mesh in order to simultaneously resolve the fine-scale structure near the submerged object and efficiently model the large-scale structure of the wake. The outer mesh is shown in Figure 2, and the inner mesh is shown in Figure 4. The submerged body is generated within this inner mesh, which is a 30-m cube centered around the submerged body. The inner mesh is translated through the flow to simulate the passage of the submerged body. The temperature, velocity, and pressure are interpolated from the larger mesh at the inner mesh boundaries. The resolution of the inner mesh matches the outer mesh resolution at these boundaries and progressively becomes more finely resolved towards the submerged body by subdividing each cell by two or four cells in each dimension. Each level of refinement is a minimum of 5 cells in width. At the body boundary, the innermost 4cm are snapped to the face to generate five layers of cells parallel to the submerged body boundary with variable thickness, finer towards the boundary. The cell at the body boundary is 0.25cm thick on average. This inner boundary is no-slip and impermeable, and the normal gradients of temperature and pressure are set to zero at the surface. The results from the inner mesh are interpolated into the outer mesh immediately around the submerged body.

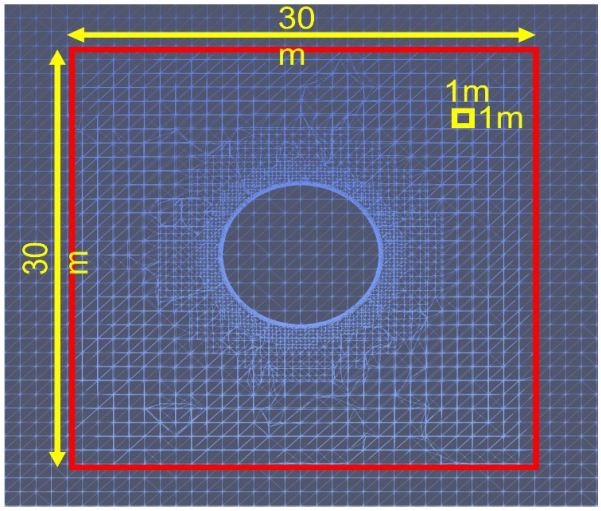

Figure 4. The vertical (x,z) section of inner mesh.

In all experiments, the submerged body is spherical with a diameter of 10m. The submerged body starts from rest at 50m from the $-x$ boundary and accelerates to maximum velocity over 2 seconds, proceeds at maximum velocity across 600m and decelerates back to rest over 2 seconds at 50m from the $+x$ boundary. The stratified wakes are then evolved for a period of 700 seconds. The inner mesh is then removed in the interest of computational efficiency. The speed of the SB (U), its depth (H), and the depth of the mixed layer (MLD) are varied between the experiments. The depths of the SB are 15m, 25m, and 40m below the surface, and the velocities of SB are 2.5m/s and 5m/s. All possible combinations are simulated both with a mixed layer extending 20m below the surface and without any mixed layer. These cases are organized in Table 1. In addition, a series of simulations are conducted with an object speed of 5m/s at a depth of 40m for variable MLD of 10m, 20m, and 40m for analyzing the influence of MLD. These cases are summarized in Table 2.

Table 1. Cases for variation in the depth and the speed of SB. Parentheses denote the total simulated time.

SB / MLD	**Speed = 2.5m/s**			**Speed = 5m/s**		
	Depth			**Depth**		
	15m	**25m**	**40m**	**15m**	**25m**	**40m**
0m	M0U2.5D15	M0U2.5D25	M0U2.5D40	M0U5D15	M0U5D25	M0U5D40
20m	M20U2.5D15	M20U2.5D25	M20U2.5D40	M20U5D15	M20U5D25	M20U5D40

Table 2. Cases for the variation in MLD.

SB / MLD	**Speed = 5m/s, Depth = 40m**
0m	M0U5D40
10m	M10U5D40
20m	M20U5D40
40m	M40U5D40

THIS PAGE INTENTIONALLY LEFT BLANK

III. RESULTS

Figure 5 illustrates the typical pattern of a simulated wake by showing the morphology of the gradient of velocity. The turbulent wake is generated shortly after the onset of SB motion and then spreads both vertically and horizontally. It takes about 100m for the wake to fully develop, so the more conspicuous structures occur beyond x=150. For instance, large vortex rings have developed, and there is very little indication of the flattening caused by stratification in these structures because the simulation is still in the near-wake stage. The velocities within the wake are still high, characteristic of the speed of the body, and the expansion is roughly isotropic. Vortices spread mainly horizontally after formation, but some signs of vertical spreading are also evident. This vertical motion is inferred as a main factor that causes a change in surface temperature.

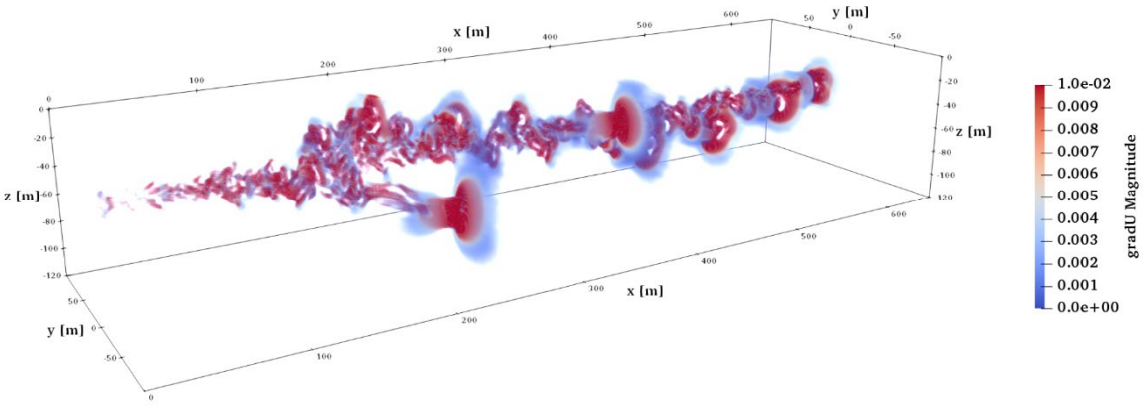

Figure 5. The gradient of velocity for a case with U = 5m/s, H = 40m, and 20m mixed layer.

To quantify the turbulence present in the wake, we use the turbulent dissipation rate, ε, which is the rate that viscosity dissipates turbulent kinetic energy and the thermal dissipation rate, χ, which is the rate that potential energy is lost through the process of thermal diffusion. The turbulent dissipation rate describes how energy is transferred from large scales to smaller scales in fluids by turbulence breaking up large structures and converting them to smaller eddies and eventually heat. We define it as follows:

$$\varepsilon = (\nu + \nu_t)[\left(\frac{\partial \mathbf{u}}{\partial x}\right)^2 + \left(\frac{\partial \mathbf{u}}{\partial y}\right)^2 + \left(\frac{\partial \mathbf{u}}{\partial z}\right)^2], \tag{3.1}$$

where the thermal dissipation rate is instead defined as

$$\chi = (K_T + \nu_t / \mathrm{Pr}_t)[(\frac{\partial T}{\partial x})^2 + (\frac{\partial T}{\partial y})^2 + (\frac{\partial T}{\partial z})^2], \tag{3.2}$$

ε and χ are used because they are indicative of the presence of microstructure, which are typically prominent in turbulent wakes and readily measurable in the ocean.

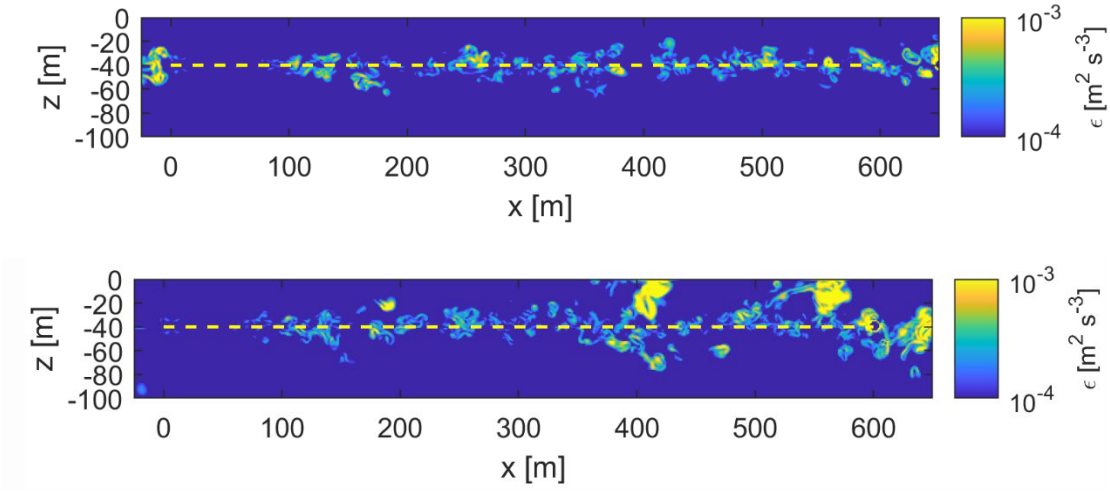

Figure 6. The vertical cross section of the turbulent dissipation rate sliced in y for a case with U = 2.5m/s and H = 40m after 700 seconds (Nt = 2.1). The upper panel presents a case without a mixed layer, and the lower panel presents a case with a mixed layer depth of 20m. The yellow dotted line indicates the path of travel of the SB. The area below z=-100m depth is removed from the plots as the wake does not reach this area.

In Figure 6, we plot the turbulent dissipation rate of an example pair of simulations with and without a mixed layer. The SB in these simulations moves at a speed of 2.5m/s and at a depth of 40m for 700 seconds. The SB travels along the dashed line, generating a turbulent wake behind it, which is visible in the figure. The wake can be easily identified by the pattern of its turbulent dissipation rate from about x=100m to

the final position of the body along the object trajectory. In the case with a mixed layer, the wake develops a stronger impact at the surface. In contrast, in the case without a mixed layer, the vertical motion of the wake is more suppressed and does not reach the surface. This suggests that a mixed layer provides less resistance to vertical motion because it is more weakly stratified than the case with constant stratification throughout.

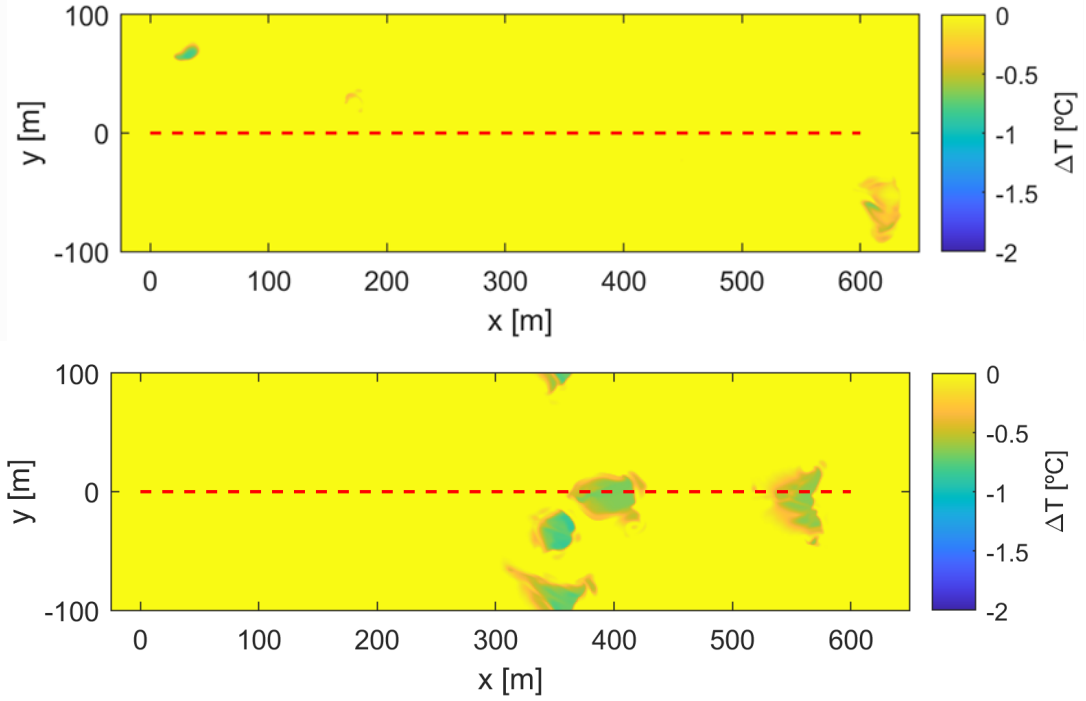

Figure 7. The temperature field at the surface for the same cases as in Figure 6. The upper panel presents a case without a mixed layer and lower panel presents a case with a mixed layer depth of 20m. The red dotted line indicates the path of the SB.

The effect of the mixed layer stratification is also evident in Figure 7, where we plot the temperature at the surface for the same cases as in Figure 6. In both panels, cold plumes are erupting to the surface, and these spots originate from upward-directed plumes generated by the wake turbulence. The plumes in the case with a mixed layer are larger and more centrally concentrated than in the case without a mixed layer. In addition, the temperature deviation of these plumes for the case with a mixed layer (about $-1\,^{o}$C)

are more extreme than that of the case without a mixed layer (About -0.5 ^{o} C). We conclude the mixed layer enhances the surface thermal signatures of the submerged body for the same reasons as described above: stronger stratification resists vertical motion and shields the surface from the wake.

A. EFFECTS OF THE VARIATION IN MLD

In Figure 8, we plot the surface temperature for simulations with varying mixed layer depth from 0m to 40m, where the speed and depth of SB are fixed at 5m/s, 40m. Overall, the surface signatures span a larger area for deeper MLD and show more extreme temperature perturbations. To investigate this, we plot the temporal averages of the thermal perturbations of the wake for these simulations in Figure 9. The area of the wake that penetrates the surface is selected by setting a temperature threshold of half of the minimum temperature at the surface. The region where the temperature is below this value is designated as the surface wake. The temperature of that region is then averaged in space and in time from 200 seconds to 700 seconds. The typical range of these temperature perturbations are shown with error-bars, which illustrate the maximum and minimum values, which are measured 200 seconds after the SB began to move. The temperature perturbation of the case without a mixed layer shows an average value of about -0.75 °C, about -0.67 °C for MLD=10m, about -0.82 °C for MLD=20m, and about -1.2 °C for MLD=40m. The background temperature of the mixed layer decreases as the mixed layer depth increases because the mixed layer dredges up colder material to the surface.

We also illustrate the area of the temperature perturbation over time, which is the integrated area at the surface where the temperature is below the same threshold. When no mixed layer is present, the size of the area where such a change occurs is relatively very small, with less than 1,000m^{2} in all time periods. In the case with MLD=10m, the wake area gradually increases as the wake continues to dredge material through the mixed layer, expanding to 4,500m^{2} by t=700s. The 20m is comparable, reaching 4,000m^{2} by t=700s, and the 40m case continues to increase rapidly from the beginning to the end, reaching 10,500m^{2} by the same time. Deeper mixed layers result in substantially

larger surface wake signatures, which would make such signals more readily observable. We can infer that with the mixed layer, which is less stratified, the buoyancy term is relatively smaller and it means vertical motion is less suppressed. On the contrary, with no mixed layer, which is more stratified, the buoyancy term is bigger and vertical motion is more suppressed. So, we can conclude the mixed layer enhances the surface thermal signatures of the submerged body.

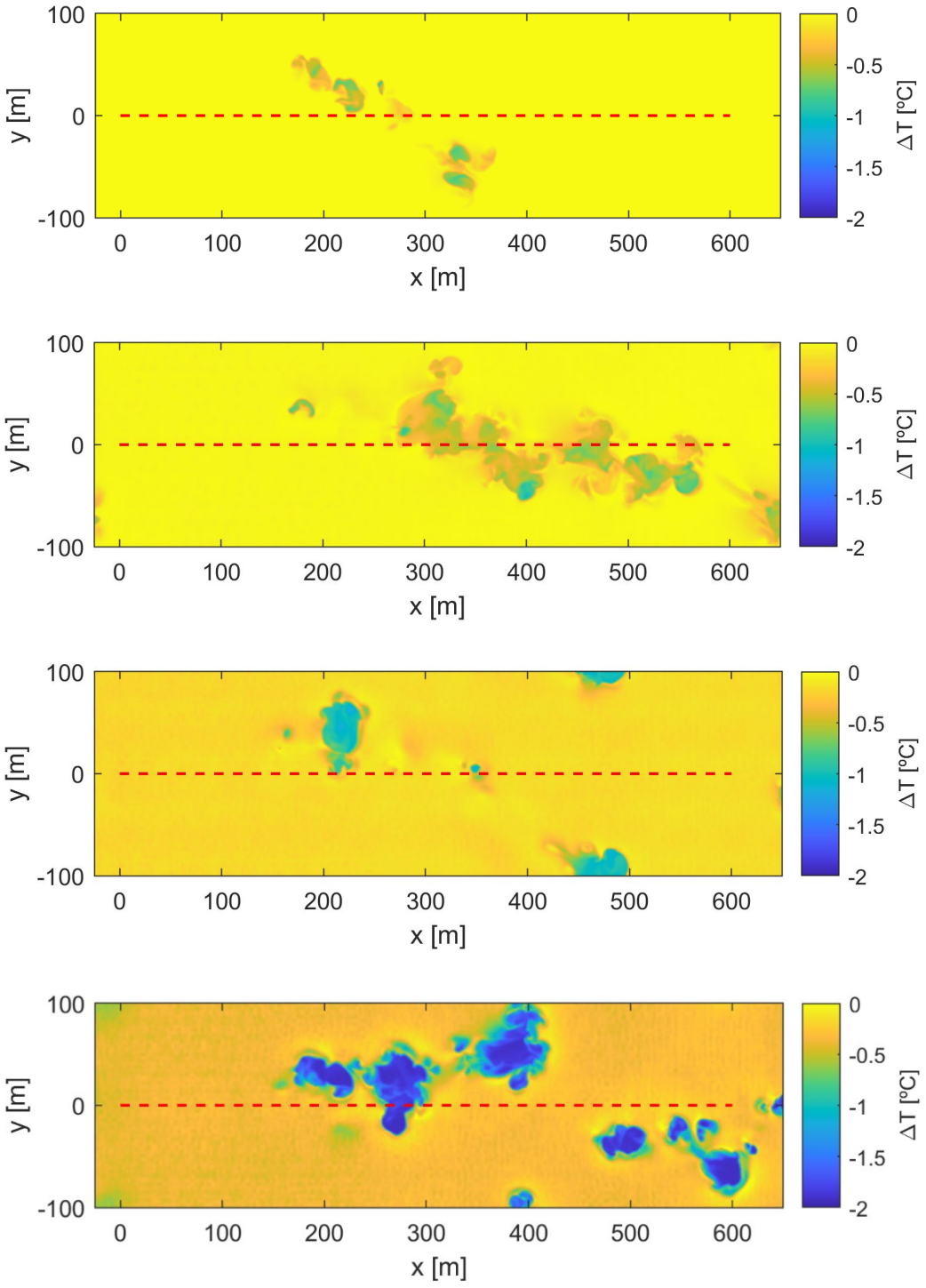

Figure 8. The temperature field at the surface for a different MLD cases with $U = 5$m/s, $H = 40$m after 700 seconds ($Nt = 2.1$). From top to bottom, the mixed layer depths are 0m, 10m, 20m, and 40m, respectively. The red dotted line indicates the path of the SB.

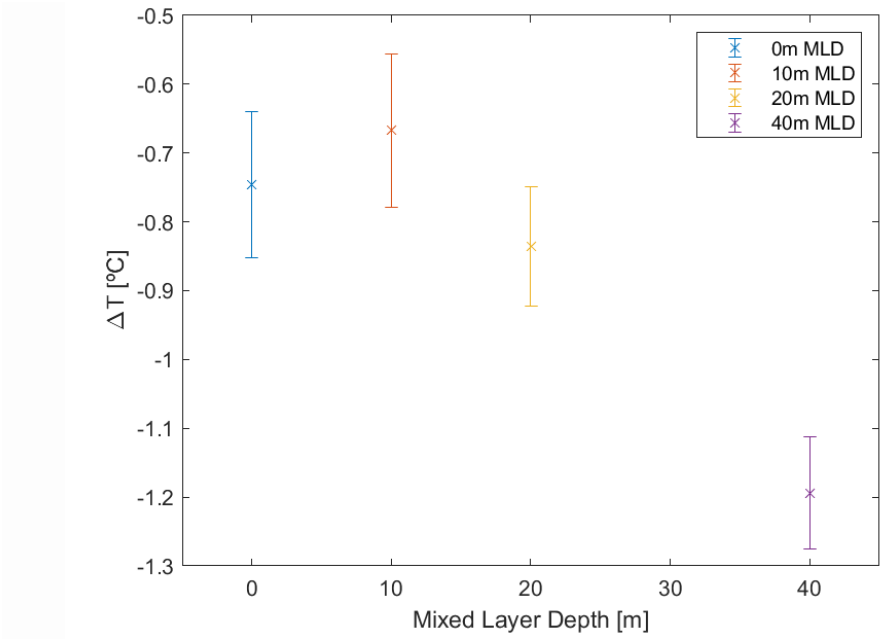

Figure 9. The average, minimum, and maximum temperature perturbation after the time from 200 seconds to 700 seconds at the different mixed layer depth for the same cases as in Figure 7.

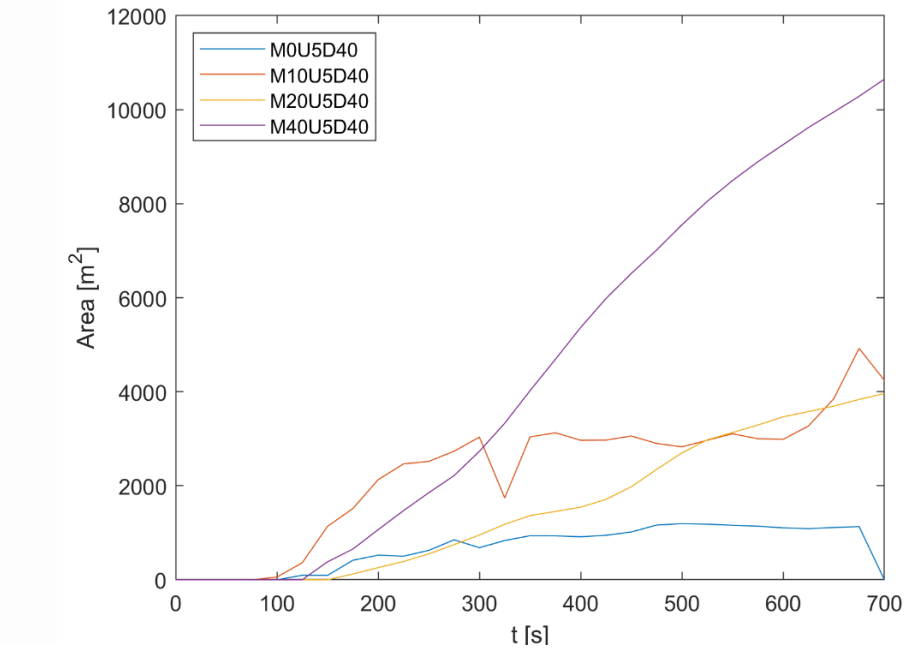

Figure 10. This plot presents the area of the temperature perturbation over time for the same cases as in Figure 7.

B. EFFECTS OF THE VARIATION IN THE SPEED AND DEPTH OF A SUBMERGED OBJECT

1. Impact on the Temperature

Figure 11 shows the temperature perturbation on the surface for simulations with the SB at different depths and the area that the wake signatures subtends over time. The mixed layer has a depth of 20m, and the speed of the SB are 2.5m/s (circles) and 5m/s (crosses). The depth of the body is represented by color, varying from 15m (red), 25m (blue), and 40m (purple). As the depth of the SB increases, the surface temperature perturbation increases, and the size of the area where such a change occurs decreases. This is likely due to the water immediately around the submerged body being colder as the depth of the body increases, and this water is then dredged up to the surface.

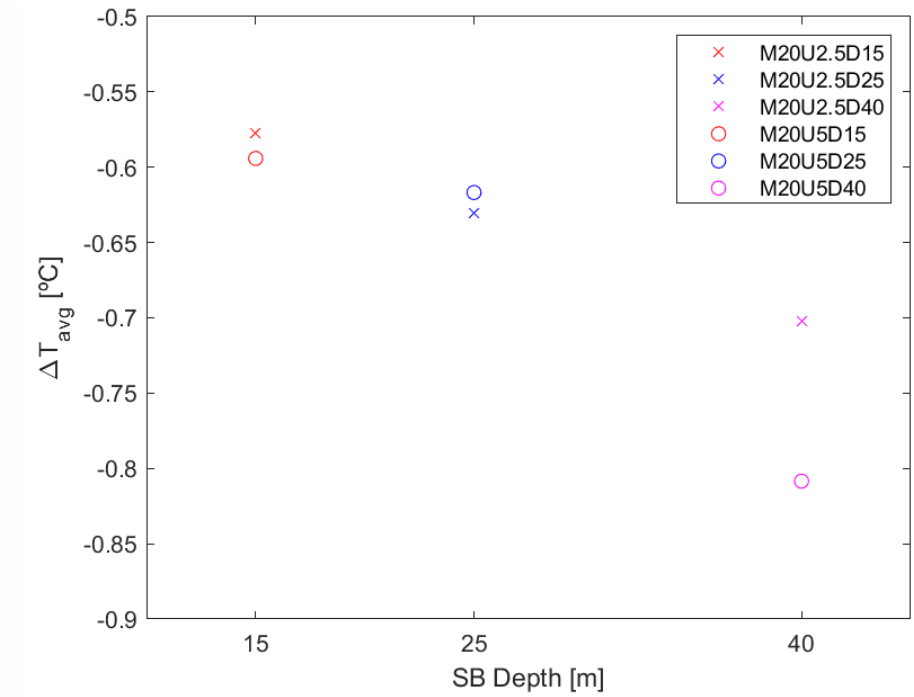

Figure 11. For the cases with MLD = 20m and the speed and depths of SB are 2.5m/s, 5m/s and 15m, 25, and 40m after 700 seconds (Nt = 2.1), this plot presents the temperature perturbation on the surface at a different depth of SB.

Figure 12 also shows the impact of the speed of the object on the temperature signal and surface wake area. There is no remarkable difference between the cases with varying speed in the cases where the object depth is small, but in the cases with H=40m, a larger surface temperature change of about 0.1 °C occurs when the speed is doubled. Conversely, the area that the wake penetrates the surface in this case shows little dependence on the object speed, where in the 15m and 25m depth cases, the wake penetrates the surface in a much larger area for a faster body (by 68% on average). However, in case with H=40m, the difference according to speed is only about 10%. Accordingly, wake generated by SB moving within or near the mixed layer forms a larger temperature change area on the sea surface, and the faster the speed, the greater the effect. However, the farther away from the mixed layer, the smaller the area and there is no change in temperature depending on the speed. This means that the closer the submarine is to the mixed layer to actively use the shadow zone, the larger the temperature change area created by the turbulence wake, which could be a disadvantage to the submarine.

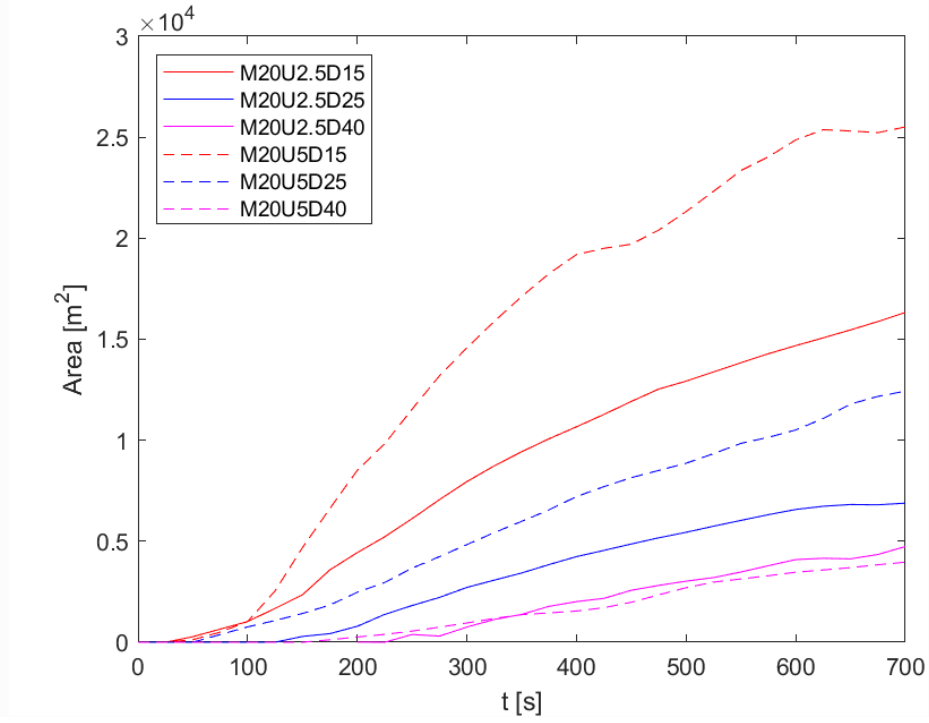

Figure 12. This plot presents the area of the temperature perturbation over time for the same cases as Figure 11.

2. Impact on the Epsilon and Chi

Figure 13 illustrates the temporal variation of net dissipation parameters $\bar{\varepsilon}$ and $\bar{\chi}$ for the same cases as presented in Figures 11 and 12. These quantities are defined as follows:

$$\bar{\varepsilon} = \frac{\int_{-100}^{100}\int_{-100}^{100}\int_{x_{\min}}^{x_{\max}} \varepsilon dxdydz}{x_{\max} - x_{\min}} \quad , \tag{3.3}$$

$$\bar{\chi} = \frac{\int_{-100}^{100}\int_{-100}^{100}\int_{x_{\min}}^{x_{\max}} \chi dxdydz}{x_{\max} - x_{\min}} \quad , \tag{3.4}$$

To meaningfully compare $\bar{\varepsilon}$ and $\bar{\chi}$ realized in different experiments, they have to be evaluated at the same time after the SB launch. Thus, the temporal records of net dissipation parameters were offset accordingly in time for the 2.5 m/s and 5.0 m/s simulations.. Cases with greater object speed show increased values of turbulent dissipation rate as is expected because of the larger Re in the system. In the case with *H*=15m case, it is about 30 times larger for U=5m/s than for U=2.5m/s. The dissipation rate slightly reduced for the *H*=25m case at about 23 times the value at for the faster SB. However, the increase in turbulent dissipation rate is much less for the case with *H*=40m case at about 2.5 times the original value. The thermal dissipation rate shows similar behavior for the deeper cases, with greater values at larger speeds for *H*=25m and *H*=40m. However, in the cases where *H*=15m case, there is no substantial effect of changing the object speed. It follows that for turbulent wakes generated within a mixed layer, there is not enough thermal variation to generate substantial levels of thermal dissipation.

Regarding the depth of the SB, both metrics show that a SB passing beneath the mixed layer produces stronger turbulence than one moving inside the mixed layer. The turbulent dissipation rates of the *H*=25m and *H*=40m cases (which are under the mixed layer for MLD=20m), are several times higher than that of the *H*=15m case. In the case

of 2.5m/s speed, for the $\bar{\varepsilon}$, 25m and 40m cases have a values 28 times and 220 times larger than 15m cases, respectively. Likewise, for the $\overline{\chi}$, in the case of 5m/s speed, 25m and 40m cases have a values 22 times and 18 times larger than 15m case, respectively. Greater speeds mitigate the effects of the SB depth, suggesting that the effect of the stratification on the generated turbulence is most prominent for lower Re. There is also notably little difference for the turbulent dissipation rate between the cases where the object is within the mixed layer, which can be explained by the local stratification. The cases within the mixed layer have essentially the same stratification as one another and therefore in situ turbulence metrics should not see substantial differences.

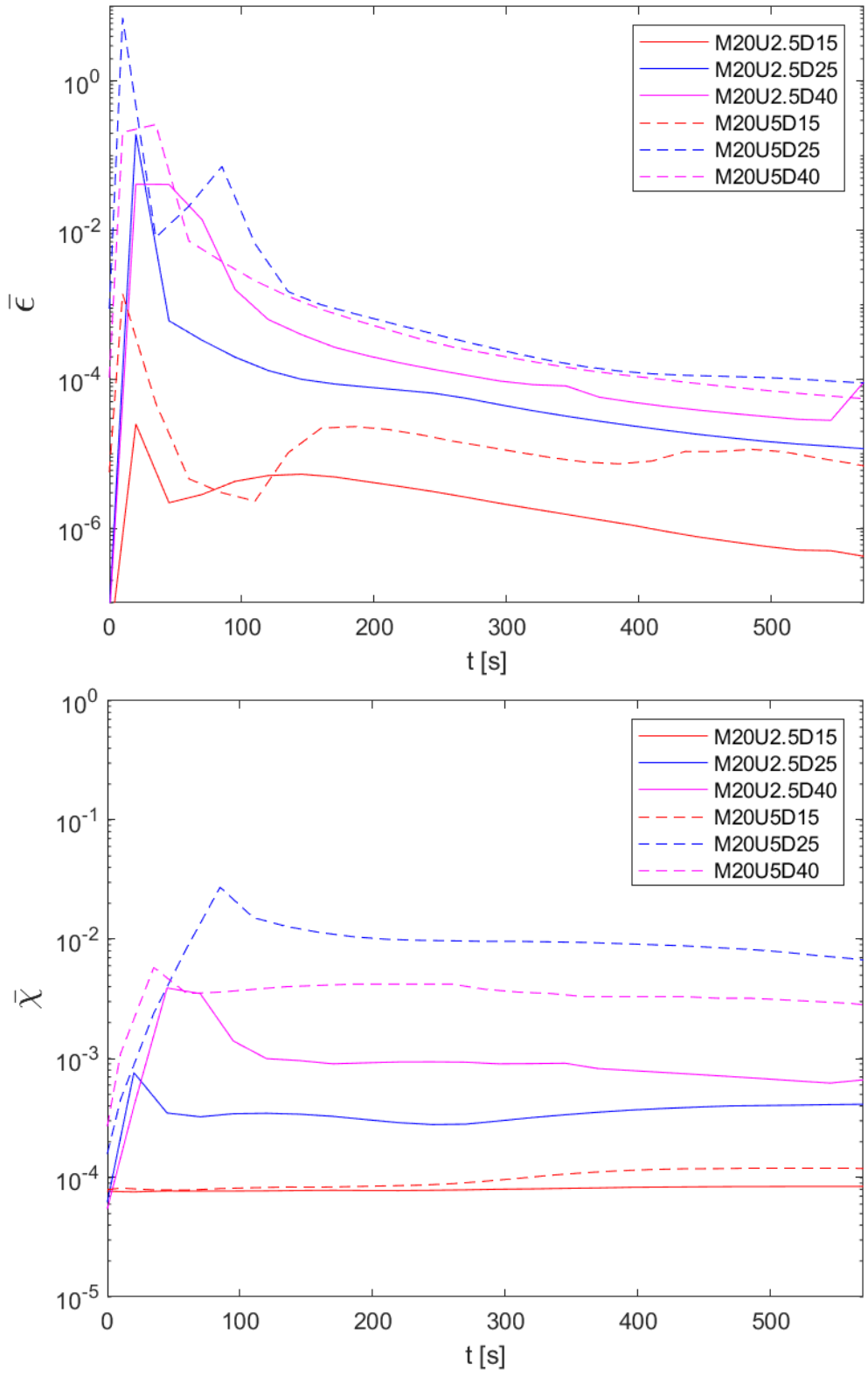

Figure 13. The $\bar{\varepsilon}$ (Upper panel) and $\bar{\chi}$ (Lower panel) are plotted as a function of time for the same cases as in Figure 12.

IV. DISCUSSION

A. CONCLUSIONS

In this study, numeral simulations were conducted using OpenFOAM to investigate how changes in MLD, speed and depth of a SB produce affect observable characteristics of the SB wake. We studied the impact of these factors on surface temperature, and the dissipation parameters $\overline{\varepsilon}$ and $\overline{\chi}$ at depth. This study has shown that the wake generated by a SB beneath a mixed layer has a greater surface temperature signature than that without a mixed layer, and the deeper the MLD, the greater the temperature change. This is because when the mixed layer is stratified much weaker than the rest of the thermocline. Therefore, the reduced buoyancy force permits fluid entering the mixed layer to penetrate further. Through variation in speed and depth of SB experiments, it was confirmed that faster SB speed results in stronger turbulence, greater temperature change and larger areas of surface wake penetration. However, through the 40m depth of case, we infer that the effect of speed is not large below a certain depth. Deeper SB trajectories result in greater surface temperature signals by dredging up colder water from the SB surroundings to the surface.

B. OPERATIONAL RELEVANCE

Detecting submarines operating in the shadow zone is one of the biggest problems in ASW. So, the surface temperature signals caused by wake, especially generated by SB under the mixed layer, are of great significance if they can be detectable using infrared detection equipment on aircraft. The temperature change of the sea surface derived in this study and the size of the area are realistically detectable. The typical temperature change at the surface for the parameters considered here range from about -0.6 °C to -1.2 °C degrees and its size from about 4,000m ^{2} to about 10,000m ^{2}. Modern airborne IR cameras can distinguish between 0.02 °C of temperature change or less and within 1m or less (Zappa, 2005). This detection method therefore represents a viable approach that avoids many issues that plague acoustic detection of submarines. The results presented in

this thesis confirmed the possibility of wake detection in the first 700s after the body passes, but these surface signatures may persist for much longer.

C. FUTURE RESEARCH

In this study, we explored wake signatures using numerical simulations and our research should be extended in other directions. An attractive alternative would be to validate our results through laboratory or field experiments designed to identify the effects that are caused by the presence of mixed layers. Specifically, in the laboratory setting, it is straightforward to establish a mixed layer with a constant temperature, salt, and density, which overlies stratified fluid. A remote-controlled SB or track-guided object could then be transported below this layer, and the temperature change that occurs could be observed using an IR camera. This could be compared to analogous situations without a mixed layer. In addition, in the same mid-latitude sea, the same experiments could be conducted in the summer, when the mixed layer is relatively shallow or may even vanish entirely, and in the winter, when it is much deeper. The resulting surface signatures of propagating SB could then be compared using IR camera based on unmanned aerial vehicles.

LIST OF REFERENCES

Brucker Kyle A., & Sarkar Sutanu. (2010). A comparative study of self-propelled and towed wakes in a stratified fluid, *Journal of Fluid Mechanics*, *652*, 373–404.

Cheng Li. G., Zhu L., Trenberth J., Mann K. E., and Abraham, J. P. (2020). Increasing ocean stratification over the past-half century, *Nature Climate Change, 10*(12), 1116–1123.

Diamessis Peter J., Spedding G. R., and Andrzej Domaradzki J. (2011). *Similarity scaling and vorticity structure in high-Reynolds-number stably stratified turbulent wakes*, Cambridge University Press.

Lin J. T., & Pao Y. H. (1974). Turbulent wake of a self-propelled slender body in stratified and non-stratified fluids*:* Analysis and flow visualization, APL/JHU POR-3586.

Lin J. T., & Pao Y. H. (1979). Wakes in stratified fluids, *Annal Review of Fluid Mechanics*,11, 317–338.

Lin J.T. and Veenhuizen, S. D. (1975), *Measurements of the decay of grid-generated turbulence in a stratified fluid*, Flow Research Note, no.85.

Maheswaran P. A., Unny V. K., Satheesh Kumar S., Uthaman C. P., and Pradeep Kumar T. (2019). Mixed layer budget terms on acoustic propagation: A study based on the butterfly track experiment in the South-Eastern Arabian Sea, *Defence Science Journal*, *69*, 1–2.

Mellor, G. L., Durbin, P. A. (1975). The structure and dynamics of the ocean surface mixed layer, J*ournal of Physical Oceanography*, 5, 718–728.

Moody Z. E., Merriam C. J., Radko T., and Joseph J. (2017). On the structure and dynamics of stratified wakes generated by submerged propagating objects, *Journal of Operational Oceanography 10*(2), 191–204.

Pao H. P., & Kao. T. W. (1977). Vortex structure in the wake of a sphere, *American Institute of Physics*, *187*(20), 6.

Redford, J. A., Lund, T. S., and Coleman, G. N. (2015). A numerical study of weakly stratified turbulent wake, *Journal of Fluid Mechanics*, 776, 568–609.

Reynolds, O. (1883). An experimental investigation of the circumstances which determine whether the motion of water shall be direct or sinuous, and of the law of resistance in parallel channel*s*, *Philosophical Transactions of the Royal Society,* 935–982.

Schooley, A. & Stewart, R. W. (1963). Experiments with a self-propelled body submerged in a fluid with a vertical density gradient, *Journal of Fluid Mechanics*, 15, 83–96.

Spalart P. R., Jou W. H., Strelets M., and Allmaras S.R.. (1997). Comments on the feasibility of LES for wings, and on a hybrid RANS/LES, *Advances in DNS/LES*, 137–147.

Spedding G. R., Browand F. K., and Fincham A. M.. (1996). Turbulence, similarity scaling and vortex geometry in the wake of a towed sphere in a stably stratified fluid, *Journal of Fluid Mechanics*, *314*(53), 103.

Spedding G. R. (1997). The evolution of initially turbulent bluff-body wakes at high internal Froude number, *Journal of Fluid Mechanics*, *337*, 283–301.

Spedding G. R. (2014). Wake signature detection, *Annual Review of Fluid Mechanics*, 46, 273–302.

Voropayev S. I., Fernando H. J. S., Smirnov S. A., and Morrison R. (2007). On surface signatures generated by submerged momentum sources, *Physics of Fluids*, *19*(7), 076603.

Weller H. G., Tabor G., Jasak H., and Fureby C. (1998). A tensorial approach to computational continuum mechanics using object-oriented techniques, *Computers in Physics*, *12*, 620.

Zappa C. J., Jessup A. T.. (2005). High-resolution airborne infrared measurements of ocean skin temperature, *IEEE*, *2* 146–150.

INITIAL DISTRIBUTION LIST

1. Defense Technical Information Center
   Ft. Belvoir, Virginia

2. Dudley Knox Library
   Naval Postgraduate School
   Monterey, California